Citation: Molecular Therapy — Oncolytics (2016) **3,** 16007; doi:10.1038/mto.2016.7
Official journal of the American Society of Gene & Cell Therapy

www.nature.com/mto

ARTICLE

A multi-antigen vaccine in combination with an immunotoxin targeting tumor-associated fibroblast for treating murine melanoma

Jinxu Fang[1], Biliang Hu[1], Si Li[2], Chupei Zhang[1], Yarong Liu[1] and Pin Wang[1–3]

A therapeutically effective cancer vaccine must generate potent antitumor immune responses and be able to overcome tolerance mechanisms mediated by the progressing tumor itself. Previous studies showed that glycoprotein 100 (gp100), tyrosinase-related protein 1 (TRP1), and tyrosinase-related protein 2 (TRP2) are promising immunogens for melanoma immunotherapy. In this study, we administered these three melanoma-associated antigens via lentiviral vectors (termed LV-3Ag) and found that this multi-antigen vaccine strategy markedly increased functional T-cell infiltration into tumors and generated protective and therapeutic antitumor immunity. We also engineered a novel immunotoxin, αFAP-PE38, capable of targeting fibroblast activation protein (FAP)-expressing fibroblasts within the tumor stroma. When combined with αFAP-PE38, LV-3Ag exhibited greatly enhanced antitumor effects on tumor growth in an established B16 melanoma model. The mechanism of action underlying this combination treatment likely modulates the immune suppressive tumor microenvironment and, consequently, activates cytotoxic $CD8^+$ T cells capable of specifically recognizing and destroying tumor cells. Taken together, these results provide a strong rationale for combining an immunotoxin with cancer vaccines for the treatment of patients with advanced cancer.

Molecular Therapy — Oncolytics (2016) **3**, 16007; doi:10.1038/mto.2016.7; published online 16 March 2016

INTRODUCTION

Therapeutic cancer vaccines and adoptive T-cell immunotherapy have been considered very attractive therapeutic approaches for the treatment of human cancer. Identification of melanoma-specific antigens, such as glycoprotein 100 (gp100), tyrosinase-related protein 1 (TRP1) and tyrosinase-related protein 2 (TRP2), has given a significant boost to the development of novel vaccines targeting melanoma.[1,2] To break tolerance to melanoma differentiation antigens, several immunization strategies have been tested, including the use of viral or bacterial vectors expressing cancer antigens, as well as HLA-binding peptides derived from tumor-specific antigens.[3–5] Immunization with lentiviral vectors (LVs) encoding TRP1 induced potent $CD8^+$ T-cell immune responses and antitumor immunity that prevented and inhibited B16 tumor growth.[6] Furthermore, delivering melanoma antigen gp100-encoded DNA vaccine into mice induced T-cell-dependent immune responses and provided protection against subsequent tumor challenge.[7,8] Notably, immunization with peptides derived from gp100 could induce a measurable antitumor immune response in patients.[9] Simultaneous immunization of mice with hgp100 and mTRP-2, two melanosome antigens, greatly protected mice from subsequent B16 melanoma tumor challenge, suggesting that immunization with the multi-antigen vaccine could be highly effective.[10]

Despite the identification of a number of tumor-associated antigens recognized by the immune system, single antigen-based cancer vaccines have yielded disappointing clinical results in the last two decades. Recently, it has become apparent that cancer vaccines alone may not work well for cancer treatment as a result of immune suppression established in the tumor lesions.[11] Thus, current cancer research has focused on vaccine-based immunotherapeutic strategies combined with conventional and novel methods of treatment.[12,13] Several combination strategies have been tested to enhance immune response and improve clinical outcomes in patients. For example, cancer vaccines have been combined with other immunotherapeutics, standard chemotherapeutic cancer drugs, targeted small-molecule drugs, local and systemic radiation of tumors, or even laser therapy.[14,15] In preclinical murine studies, chemotherapy agents, including cyclophosphamide, doxorubicin, paclitaxel, and docetaxel,[16] enhanced antitumor immune responses to a whole tumor-cell vaccine.[17] Combination of LV immunization and low-dose chemotherapy, or PD-1/PD-L1 blocking, primed self-reactive T cells and induced antitumor immunity.[18] A small trial combining granulocyte–macrophage colony-stimulating

The first two authors contributed equally to this work.
[1]Mork Family Department of Chemical Engineering and Materials Science, University of Southern California, Los Angeles, California, USA; [2]Department of Pharmacology and Pharmaceutical Sciences, University of Southern California, Los Angeles, California, USA; [3]Department of Biomedical Engineering, University of Southern California, Los Angeles, California, USA. Correspondence: P Wang (pinwang@usc.edu)
Received 20 January 2016; accepted 25 January 2016

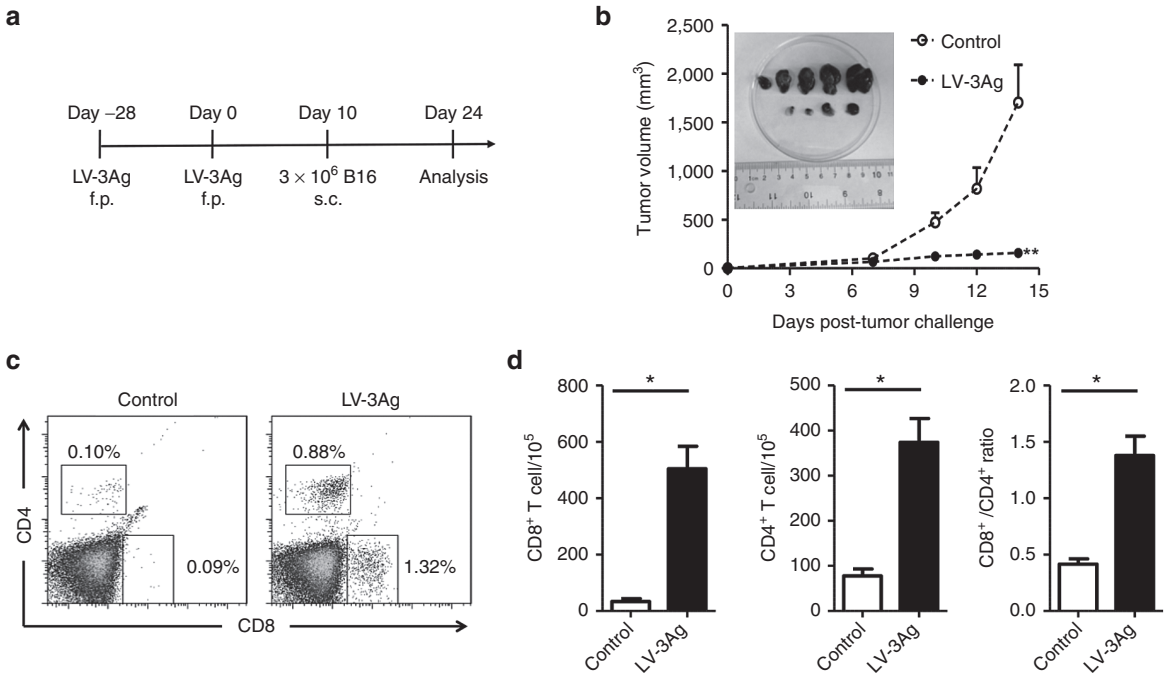

Figure 1 Protection of mice against B16 melanoma tumor cell challenge after immunization with the LV-3Ag. (**a**) Schematic representation of the immunization protocol. Mice were immunized at day −28 with the vesicular stomatitis virus glycoprotein-enveloped recombinant vector LV-3Ag and boosted at day 0 with the SVGmu-enveloped vector. Ten days after boost immunization, mice were challenged subcutaneously with B16-F10 cells (3×10^6). Tumor growth was monitored every other day, and tumor-infiltrating T cells were detected at day 24. (**b**) Tumor growth curve of the transplanted B16-F10 cells in C57BL/6 mice vaccinated as described above. Data are presented as mean tumor volume ± standard error of the mean (SEM) at indicated time points. The inserted picture shows tumor tissues at day 24 after boost immunization. (**c**) Representative fluorescence-activated cell sorting plots for measuring the population of $CD8^+$ and $CD4^+$ T cells in the tumor tissue. (**d**) The percentages of $CD8^+$ and $CD4^+$ tumor-infiltrating T cells were determined at day 24 after boost immunization ($n = 5$, error bars indicate SEM; $^*P < 0.05$, $^{**}P < 0.01$). Data are representative of two independent experiments.

factor-secreting tumor cell vaccines with CTLA4 blockade was found to increase inflammatory infiltrates and tumor regression.[19] However, the combination of cancer vaccine and immunotoxins, which are highly specific and very potent molecules that kill tumor cells directly at very low concentrations, has been much less studied.

Tumors consist of heterogeneous populations of cells, including both transformed and untransformed cells, which vary among different tumors at different stages of tumorigenesis.[20] However, they do contain some regular cell types, such as infiltrating inflammatory and immune cells, endothelial cells and myeloid-derived suppressor cells (MDSCs), pericytes, and tumor-associated fibroblasts (TAFs). TAFs, a heterogeneous fibroblast population phenotypically distinguished from normal fibroblast cells, are primarily responsible for the synthesis, deposition, and remodeling of the extracellular matrix, as well as production of growth factors, cytokines, and chemokines that promote tumor growth and metastasis.[21,22] These cells selectively express high levels of fibroblast activation protein (FAP), a type II transmembrane cell surface serine protease of the dipeptidyl peptidase IV family.[23,24] As FAP-expressing fibroblast cells have been shown to suppress antitumor immunity,[25] this protein has gained great attention for targeted therapy in recent years.[26] In our previous study, we have shown that depletion of FAP-expressing stromal cells reduced the recruitment of infiltrating tumor-associated macrophages, attenuated angiogenesis to deprive tumor cells of required nutrients and oxygen, and inhibited tumor cell growth.[27] In addition, we and others[25] have shown that depletion of FAP-positive stromal cells can also modulate the expression profile of growth factors, cytokines, and chemokines, thus altering the tumor microenvironment.

In this study, we tested the efficacy of LV immunization with a combination of three antigens, gp100, TRP1, and TRP2 (LV-3Ag), in tumor prevention and inhibition in a prophylactic and therapeutic B16 melanoma model. We also investigated the efficacy of combining αFAP-PE38 and LV-3Ag vaccine (hereinafter termed as "combination treatment") in the same mouse model. Finally, we explored the mechanism underlying the enhanced antitumor activity of the combination treatment.

RESULTS

Immunization with LV-3Ag conferred antimelanoma tumor activity in a prophylactic model

We first investigated the efficacy of lentiviral vaccine LV-3Ag in tumor protection in a prophylactic B16 melanoma model. C57BL6 mice were primed with a subcutaneous (s.c., footpad) injection of the mixed LV-3Ag vectors pseudotyped with vesicular stomatitis virus glycoprotein (5×10^6 transduction units for each antigen), followed by a boost injection consisting of the mixed LV-3Ag vector pseudotyped with a dendritic cell-targeted glycoprotein derived from sindbis virus (SVGmu) (5×10^6 transduction units for each antigen). Mice vaccinated with phosphate-buffered saline (PBS) at all injection points were used as controls. The mice were challenged 10 days post-boost immunization by s.c. (flank site) injection of B16-F10 melanoma cells (3×10^6). When the tumors reached a certain size, the mice were euthanized, and spleen cells were harvested for further analysis (Figure 1a). A strong tumor-protective immunity was observed in the LV-3Ag-immunized group. One mouse rejected tumor completely, and the remaining animals had significant suppression of tumor size compared with mice in the control groups (Figure 1b), confirming

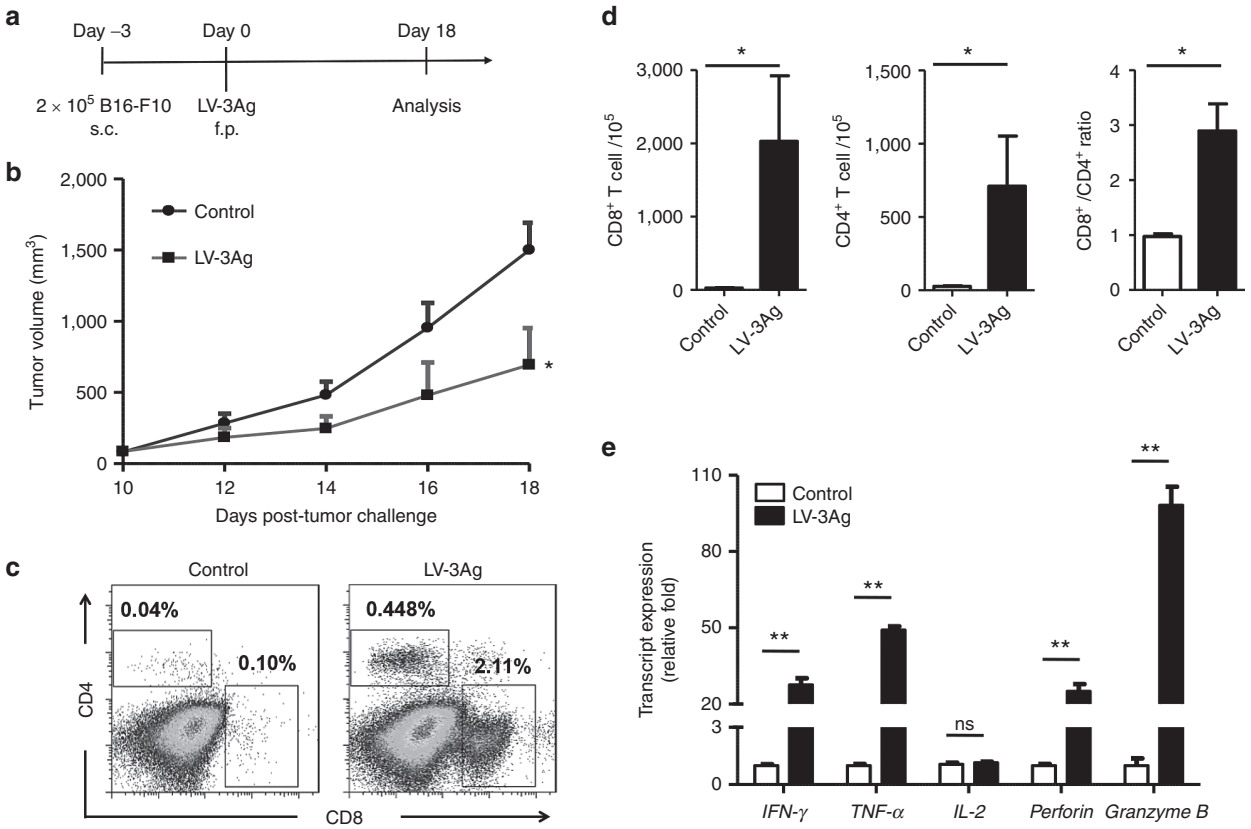

Figure 2 Therapeutic efficacy of LV-3Ag immunization against B16 melanoma tumor. (**a**) Schematic diagram of the experimental protocol for tumor challenge and LV-3Ag vaccination. Mice were s.c. challenged with 2×10^5 of B16-F10 tumor cells and then immunized at day 3 via f.p. injection of LV-3Ag (10^7 transduction units). (**b**) Tumor growth curve of s.c. transplanted B16-F10 cells in mice vaccinated as described above. Tumor growth was measured every other day, and mice were euthanized when tumor size in control groups reached around 2,000 mm^3. Data are presented as mean tumor volume ± standard error of the mean (SEM) at indicated time points. (**c**) Representative fluorescence-activated cell sorting plots for measuring the population of $CD8^+$ and $CD4^+$ T cells in the tumor tissues. (**d**) The percentage of infiltrating $CD8^+$ and $CD4^+$ T cells. (**e**) The mRNA expression levels of IFN-γ, TNF-α, IL-2, perforin, and granzyme B in tumor tissues harvested at day 18. Total RNAs extracted from tumor tissues in each group were pooled, and mRNA expression levels were determined by real-time reverse transcription–PCR. Graph depicts relative levels of mRNA after normalizing to GAPDH mRNA levels ($n = 5$, error bars indicate SEM; $^*P < 0.05$, $^{**}P < 0.01$). Data are representative of two independent experiments.

that multi-antigen LV-3Ag immunization could be directly correlated with tumor growth-inhibiting immune response.

It has been well established that both cytotoxic $CD8^+$ T cells and helper $CD4^+$ T cells are involved in antitumor immunity.[28,29] Therefore, we next analyzed the infiltration of $CD4^+$ and $CD8^+$ T cells in tumor tissues upon immunization with LV-3Ag. Tumor cell samples from control and LV-3Ag-immunized mice were collected, stained, and subjected to flow cytometric analysis. As shown in Figure 1c, compared with the control mice, immunization resulted in increased infiltration of $CD4^+$ and $CD8^+$ T cells in tumor tissues harvested from LV-3Ag-immunized mice. Further calculation showed that LV-3Ag immunization markedly increased the number of T cells infiltrating tumor lesions and also enhanced the ratio of $CD8^+/CD4^+$ T cells (Figure 1d). This suggests that both cytotoxic and helper T cells infiltrated local tumor tissue in response to LV-3Ag immunization.

LV-3Ag immunization potently inhibited tumor growth in a therapeutic model

We also investigated whether LV-3Ag immunization could potently inhibit tumor growth in a therapeutic model. Immunization was carried out three days after inoculation of B16-F10 tumor cells (0.5×10^6), and the tumor volume was measured every other day starting from 10 days postinoculation (Figure 2a). Tumor-bearing mice therapeutically vaccinated with LV-3Ag showed significantly slower tumor growth when compared to control group (Figure 2b). Similar to results observed in the prophylactic model, we observed a significantly increased number of infiltrated $CD4^+$ and $CD8^+$ T cells, as well as enhanced ratio of $CD8^+/CD4^+$ T cells, in the tumors harvested from LV-3Ag-immunized mice compared to control mice (Figure 2c,d).

Based on LV-3Ag immunization-induced enhancement of tumor-infiltrating lymphocytes, we further investigated whether the expression of cytokines with antitumor activities changed in the tumor microenvironment in response to LV-3Ag immunization. We found that tumor tissues isolated from LV-3Ag-immunized mice exhibited significantly upregulated levels of T-cell activation-associated cytolytic cytokines and enzymes, including IFNγ, TNF-α, perforin, and granzyme B, when compared to mice receiving PBS injection. However, no significant difference in IL-2 mRNA expression was observed (Figure 2e).

αFAP-PE38 treatment significantly enhanced the therapeutic activity of LV-3Ag immunization

Selective expression of FAP was identified to be associated with tumor stromal cells, making it an ideal target for immunotherapy.[26,30] We have recently found that αFAP-PE38 treatment altered

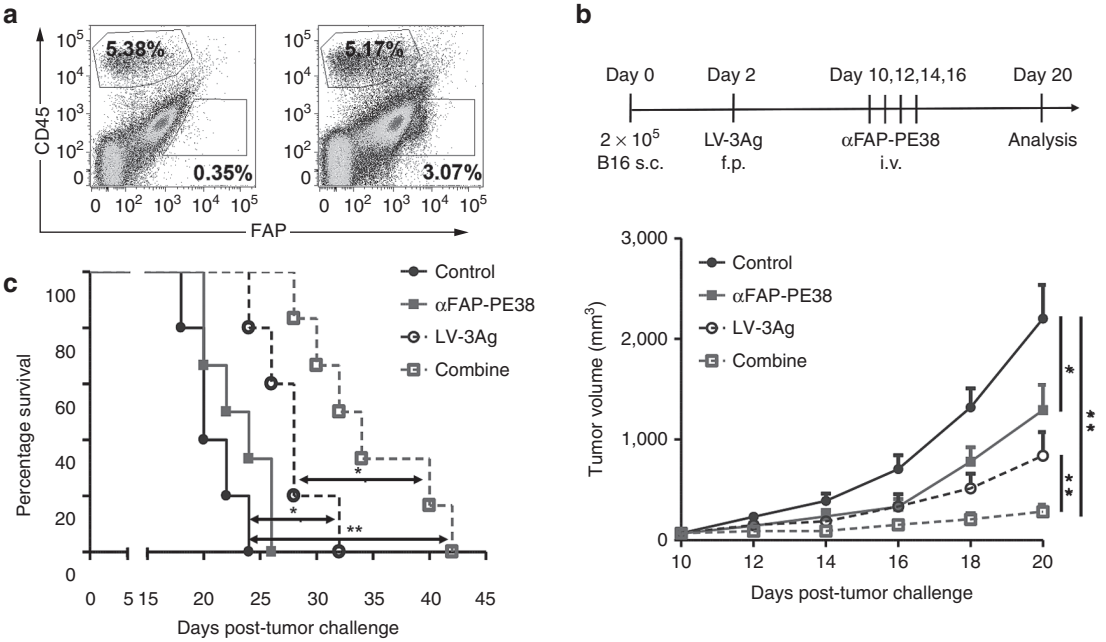

Figure 3 The combination of LV-3Ag immunization and αFAP-PE38 treatment increased antitumor activity. (**a**) Representative fluorescence-activated cell sorting plots for the population of $CD45^{-}FAP^{+}$ stromal cells in B16 tumor. (**b**) Tumor growth curves in B16-bearing mice. Mice were s.c. challenged with 2×10^5 B16-F10 tumor cells at right flank and then immunized at day 3 via f.p. injection of LV-3Ag (10^7 transduction units) At day 10, αFAP-PE38 treatment was initiated, and a total of four injections were administered on the indicated dates. Tumor volume was measured every other day, and mice were euthanized when the tumor volume in control groups reached around 2,000 mm^3 ($n = 10$). (**c**) Mouse survival was calculated using the Kaplan-Meier method (error bars indicate standard error of the mean; $^*P < 0.05$, $^{**}P < 0.01$). Data are representative of two independent experiments.

levels of various growth factors, cytokines, chemokines, and matrix metalloproteinases in the tumor microenvironment.[27] Based on the existing $CD45^{-}FAP^{+}$ stromal population in the B16 melanoma model, as shown in Figure 3b, we hypothesized that αFAP-PE38 treatment might have an additive, or synergistic, effect on the antitumor activity of LV-3Ag immunization. Therefore, the efficacy of LV-3Ag immunization combined with αFAP-PE38 (hereinafter termed "combination treatment") treatment was evaluated. C57BL6 mice were injected s.c. with B16-F10 tumor cells (2×10^5) on day 0 and received no treatment, αFAP-PE38 immunotoxin only, vaccine only, or vaccine plus αFAP-PE38 treatment (Figure 3b). The combination treatment showed a statistically significant antitumor effect compared to no treatment ($P < 0.0001$), vaccine alone ($P < 0.001$), or αFAP-PE38 alone ($P < 0.001$) at day 20 (Figure 3b). Importantly, tumor progression was delayed in >80% of mice receiving the combination treatment. Furthermore, the survival study showed that the group receiving combination treatment had a median survival of 31 days (tumor size of 2,000 mm^3 was used as a surrogate endpoint of survival) and lived significantly longer than mice treated with αFAP-PE38 alone, vaccine alone, or those in the control group (Figure 3c).

Combination treatment greatly reduced cell proliferation and induced apoptosis

We next explored the mechanism underlying significantly improved tumor growth inhibition *in vivo* by combination treatment. Tumors were excised from the treated mice and subjected to H&E staining, immunohistochemistry staining of Ki-67 for cell proliferation analysis, and terminal deoxynucleotidyl transferase dUTP nick end labeling (TUNEL) assay for cell apoptosis analysis. Immunohistochemical analyses of tumor tissues revealed that the tumors isolated from mice receiving combined αFAP-PE38 and LV-3Ag treatment presented a dramatically decreased tumor cell proliferation rate (Figure 4a,b). Intratumoral proliferative index had decreased by 18.91% in the αFAP-PE38-treated group, as compared to the control group. LV-3Ag immunization resulted in a 28.96% decrease in intratumoral proliferative activity compared with controls. However, the combination treatment resulted in a 48.82% decrease in intratumoral proliferation compared with the control group and each single treatment group. Intratumoral apoptosis in tumor tissues was examined, and the apoptotic index was found to be significantly increased in the combined treatment group, as compared to the αFAP-PE38-treated group, LV-3Ag-immunized group, or control group (Figure 4a,c).

The combination treatment modulated infiltration of immune cells into tumor tissues

To understand the mechanism(s) of action underlying apparent enhanced antitumor activity of the combination treatment approach, we analyzed the effects of single treatment or combined therapy on tumor-infiltrating immune cells harvested from treated mice (day 20). No significant changes in tumor-associated macrophages (TAMs) or natural killer (NK) cells were observed in αFAP-PE38- and LV-3A-treated (either alone or in combination) primary tumors compared with the other therapeutic groups (data not shown). The ratio of $CD8^{+}$ T cells versus T regulatory cells (Treg) has been linked to both cancer progression[31,32] and therapeutic outcomes in mice and humans.[33,34] We found that combination treatment, but not any single treatment, significantly increased CD8/Treg ratios within the tumor, which has also been previously described as predictive of therapeutic efficacy in the B16 melanoma model[35] (Figure 5a). Similarly, we observed significantly increased CD4/Treg ratios within the tumor in the combination treatment group (Figure 5b). We next analyzed the activation state of tumor-infiltrating T cells among the different treatment groups by measuring the expression of PD-1 protein, a key coinhibitory

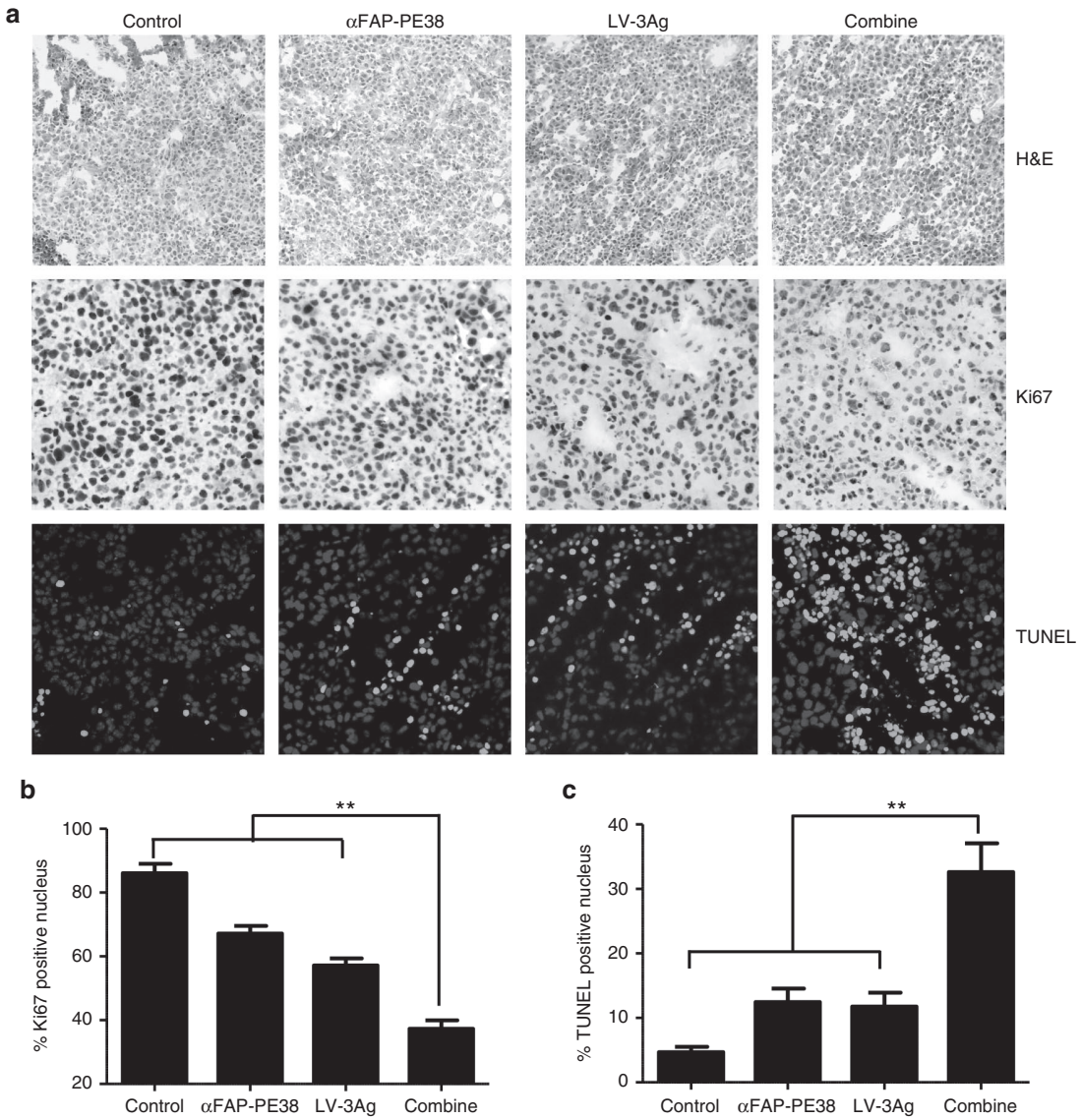

Figure 4 The combination of LV-3Ag immunization and αFAP-PE38 treatment inhibited tumor cell proliferation and induced apoptosis *in vivo*. Effects of LV-3Ag and αFAP-PE38 treatments on intratumoral proliferative and apoptotic activities. (**a**) Representative images of hematoxylin and eosin (H&E) staining (magnification: ×200) and immunohistochemistry for analysis of cell proliferation marker (Ki-67), as well as apoptosis (terminal deoxynucleotidyl transferase dUTP nick end labeling (TUNEL) assay), in tumors removed from the treated mice in Figure 3b (magnification: ×400). (**b**) Quantification of the number of Ki-67-positive proliferative cells shown in (**a**). To quantify Ki-67-positive cells, 10 fields were randomly chosen to count the percentage of Ki-67-positive nuclei in the nuclear staining area. Data are represented as mean ± SD ($n = 3$). (**c**) Quantification of TUNEL-positive apoptotic tumor cells. Images were randomly selected from 10 fields in each treated group. Within one field, the number of TUNEL-positive nuclei in the nuclear staining was calculated. The data are expressed as % total nuclear area stained by TUNEL in the field. Data are presented as mean ± SD ($n = 3$).

receptor on tumor-infiltrating T cells. The combination treatment group showed a significantly lower percentage of PD-1-expressing $CD8^+$ cells in tumors compared with LV-3Ag alone, αFAP-PE38 alone, or the control group (Figure 5c). This effect occurred specifically in the $CD8^+$ T-cell compartment, as shown by the unchanged percentage of PD-1-expressing $CD4^+$ T cells in tumors upon treatment (Figure 5d).

In addition to Treg cells, MDSCs, another major component of the immune suppressive tumor microenvironment, can dampen T-cell activity within tumors, thereby favoring tumor progression.[36] We therefore assessed the effects of combined therapy on MDSCs. Single LV-3Ag vaccination or αFAP-PE3 treatment slightly increased the ratio of $CD8^+$ T cells to MDSCs within the tumor (Figure 5e). In contrast, combination treatment significantly increased CD8/MDSC ratios compared with LV-3Ag vaccination alone, αFAP-PE3 treatment alone, or no treatment. Furthermore, the combined therapy also significantly increased the ratio of CD4/MDSC in tumors (Figure 5f).

The combination treatment altered cytokine profile and fostered a local immune stimulatory tumor microenvironment

To further substantiate the observed changes of tumor microenvironment, we next examined the gene expression of T-cell activation markers and associated cytolytic cytokines in tumor-bearing mice by quantitative reverse transcription–PCR (RT–PCR) (Figure 6). Inducible T-cell costimulator (ICOS), a T-cell activation marker, was significantly increased in the tumors after treatment with LV-3Ag plus αFAP-PE38, compared with αFAP-PE38 alone, LV-3Ag alone, or untreated tumors. More importantly, tumors from mice treated with the combination treatment had significantly elevated mRNA levels of

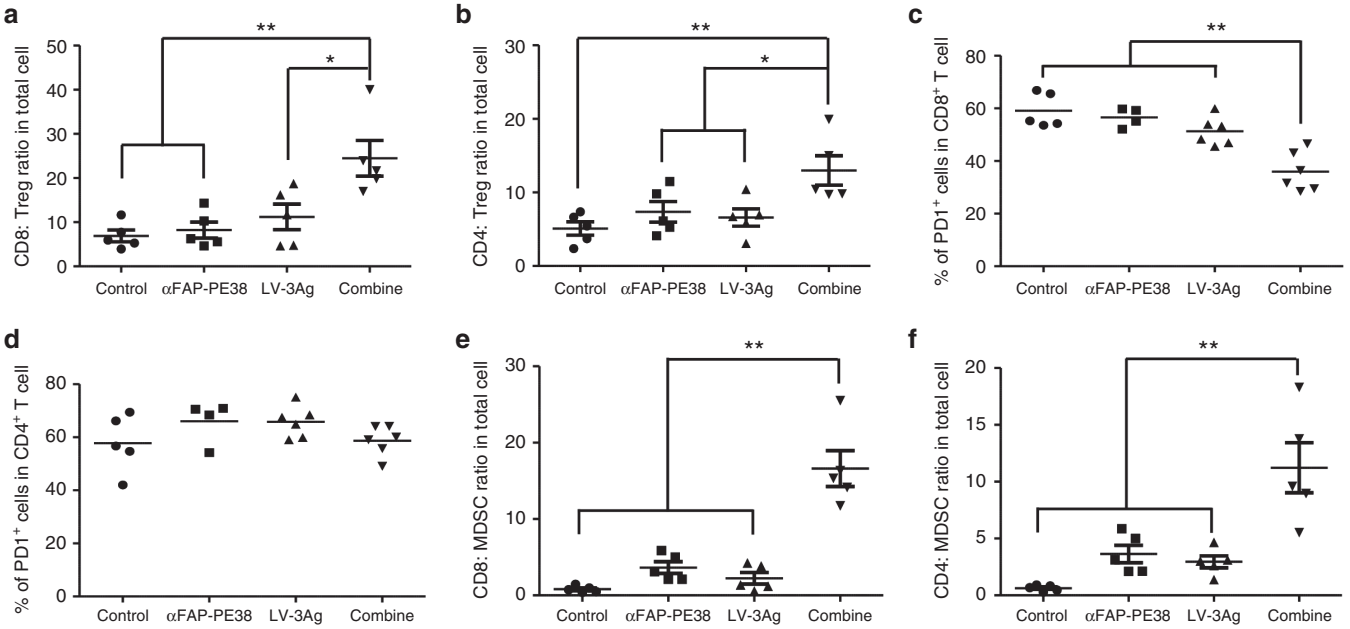

Figure 5 LV-3Ag immunization in combination with depletion of FAP$^+$ stromal cells enhanced tumor-infiltrating T cells and increased the ratio of T effector cells versus Treg cells or myeloid-derived suppressor cells within tumor. The population of tumor-infiltrating lymphocytes in B16 tumor tissues (day 20) as described in Figure 3b. Cells were purified from the harvested single-cell suspension by Percoll density-gradient separation, stained by various makers, and analyzed by flow cytometry for the composition of various subsets of immune cells. (**a**,**b**) Percentages of CD8$^+$ and CD4$^+$ T cells expressing PD-1 within CD45$^+$ TILs. (**c**,**d**) The ratios of CD8$^+$ and CD4$^+$ T cells to CD4$^+$CD25$^+$FoxP3$^+$ Treg cells. (**e**,**f**) The ratios of CD8$^+$ and CD4$^+$ T cells to Lin$^-$CD11b$^+$Gr-1$^+$ MDSCs. The data shown were individually analyzed from mice that received the indicated therapy, and *t*-tests were performed to determine the statistical significance between samples ($n = 5$, error bars indicate standard error of the mean; $^*P < 0.05$, $^{**}P < 0.01$). Data are representative of two independent experiments.

perforin, a protein present in the cytoplasmic granules of CD8$^+$ cytotoxic T lymphocytes (CTLs), TRAIL, a stimulator of apoptosis in transformed cells,[37] and TNF-α, which can induce acute and hypoxic death of both cancer and stromal cells,[25] when compared with those from control, LV-3g-immunized-, or αFAP-PE38-treated mice. IL-12p70 heterodimer, composed of IL-12p35 and IL-12p40 subunits, is a major Th1-driving cytokine, promoting cell-mediated tumor immunity.[38,39] Combination treatment also significantly increased mRNA level of IL-12p35, but not IL-12p40. IL-2 has been suggested to boost antitumor T-cell responses by acting as a second costimulatory signal during CTL activation.[40] αFAP-PE38 treatment increased IL-2 levels, and it was more profound in the combination treatment group. IL-2 expression was slightly increased in the αFAP-PE38 treatment group, and such upregulation was more profound in the combination treatment group. No significant change was observed in any group for TGF-β expression.

DISCUSSION

Here, we have used a new strategy to improve the immunogenicity of cancer vaccines by codelivering a mixture of tumor differentiation antigens, including gp100, TRP1, and TRP2 (LV-3Ag). LV-3Ag immunization displayed significant antitumor activity, as evidenced by the almost completely abolished tumor formation in a prophylactic B16 melanoma model. Notably, LV-3Ag immunization greatly increased the number of tumor-infiltrating T lymphocytes, as well as the expression of cytolytic proteins and cytokines with antitumor activities. Furthermore, combination treatment with LV-3Ag and αFAP-PE38 demonstrated remarkable antitumor effects in established tumors, a paradigm close to the clinical situation. Underlying this effect, we observed the inhibition of cell proliferation, evidence of more apoptotic cells, and significantly increased ratio of CD8$^+$ T cells relative to Tregs and MDSCs in tumors from the group that received combination treatment. Finally, the genes of cytolytic cytokines and enzymes, such as IL-2, IL-12, TNF-α, and perforin, had higher expression levels in the group treated with LV-3Ag plus αFAP-PE38.

Choice of antigen is one of the critical steps in tumor vaccine design. However, because of heterogeneous expression of antigens in tumor, most single-antigen vaccine therapies have resulted in limited therapeutic efficacy. Thus, targeting multiple distinct tumor-associated antigens in a single vaccination regimen would likely elicit additive or synergistic polyclonal T-cell responses able to prevent tumor escape from antigen loss, and thus confer more effective antitumor efficacy. Indeed, LV-3Ag vaccination prevented subsequent tumor challenge and also greatly inhibited the growth of established tumor in mice. Generation of a strong and effective antitumor immune response in tumor-bearing patients, which is the hallmark of successful cancer vaccination, requires the use of a powerful immunization strategy that can achieve the highest efficacy. Compared to DNA vaccines, which require multiple inoculations or the use of adjuvants to improve their efficacy, lentiviral vaccines, which can infect both dividing and nondividing cells, are considered to be a stronger vaccine carrier, yielding more effective immune responses.[41]

Immunotherapy for solid tumors has shown some promising outcomes in preclinical and early clinical studies. However, the efficacy of immunotherapy in eradicating established tumors remains challenging.[42,43] Our results showed that LV-3Ag immunization was less effective in inhibiting growth of established tumor growth in a therapeutic model when compared to its ability to block tumor formation in a prophylactic model. Such differences most likely result from the dynamic and complex microenvironment in the tumor. In particular, TAFs, the most predominant cell type in solid tumors, play a critical role in building an immunosuppressive tumor microenvironment

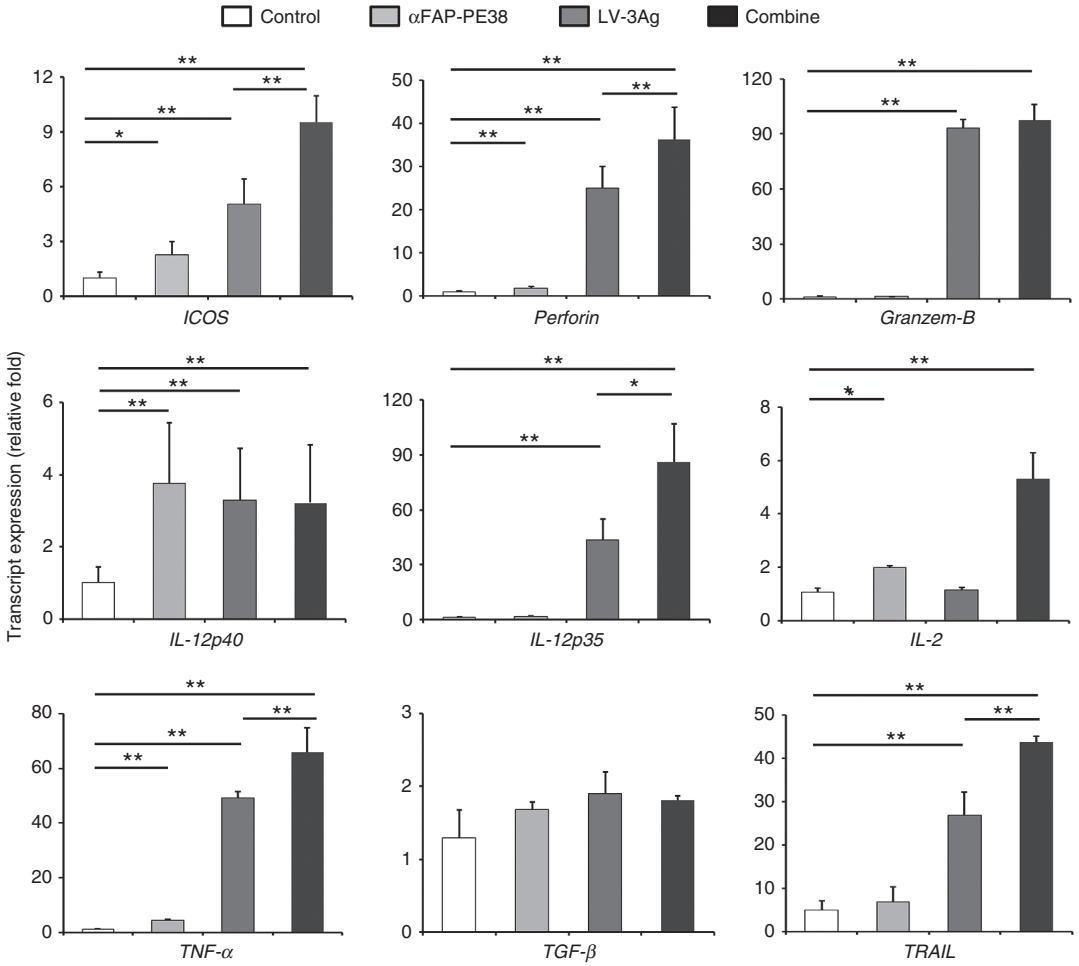

Figure 6 LV-3Ag immunization and depletion of FAP$^+$ stromal cells altered the tumor immune microenvironment. Analysis of mRNA expression levels of *ICOS, perforin, granzyme B, IL-12p35, IL-12p40, IL-2, TNF-α, TGF-β*, and *TRAIL* from tumor tissues (day 20), as described in Figure 3b. Five tumors from each group were resected, homogenized and pooled. Total RNA was extracted, and the mRNA expression levels were determined by real-time reverse transcription–PCR. Graph depicts relative levels of mRNA after normalizing to GAPDH mRNA levels (mean ± SEM; *$P < 0.05$, **$P < 0.01$).

able to facilitate tumor growth and metastasis through secreting a range of paracrine factors. For example, TAFs can disrupt IL-2 production of activated T cells and subsequently suppress proliferation in a contact-dependent manner.[44] A subset of TAFs was found to constitutively express programmed death ligands 1 and 2 (PD-L1 and PD-L2), which can bind to the programmed death 1 receptor (PD-1) on T cells and impair T-cell function.[45] Additionally, TAFs have also been suggested to further bolster the immunosuppressive microenvironment by the recruitment of MDSCs and Tregs.[46] TGF-β, which is secreted by TAFs, also contributes to the expansion of naturally occurring Tregs.[47] Based on the evidence in these previous reports, we asked if targeting TAFs would improve the efficacy of LV-3Ag immunotherapy. Indeed, the combination treatment was able to alter the tumor microenvironment, increase the ratio of T cells to both Tregs and MDSCs, and yield significantly improved therapeutic outcome. These findings suggest that the administration of αFAP-PE38 could attenuate the immunosuppressive tumor microenvironment, resulting in the activation of more CTLs and facilitating the release of cytolytic cytokines to produce better antitumor efficacy with combination treatment. In addition, we also found that combined treatment decreased PD-1 expression in tumor-infiltrating CD8$^+$ T cells. PD-1 is usually elevated in tumor-infiltrating CD8$^+$ T cells, which impairs these cells to mount antitumor immune responses. It has been recently reported that VEGF produced in the tumor microenvironment enhanced the expression of PD-1 and other inhibitory checkpoints involved in CD8$^+$ T-cell exhaustion.[48] We have previously shown that immunotoxin αFAP-PE38 reduced the level of VEGF in the tumor microenvironment,[27] suggesting that the observed reduction of PD-1 in CD8$^+$ T cells could be partially due to the variation of VEGF. Thus, our current study not only provided proof-of-principle for the use of multiple tumor antigens toward the improvement of antitumor efficacy, but also highlighted the potential of targeting TAFs to improve current immunotherapeutic approaches against cancer.

MATERIALS AND METHODS

Mice and cell line

C57BL/6 mice were purchased from Charles River Laboratories (Wilmington, MA). All animal experiments and protocols were performed according to the guidelines set by the NIH and the University of Southern California on the Care and Use of Animals. B16-F10 and 293T cells were purchased from ATCC (Manassas, VA) and cultured in high-glucose Dulbecco's modified Eagle medium (Hyclone, Logan, UT) with L-glutamine (Hyclone Laboratories, Omaha, NE) supplemented with 10% fetal bovine serum (Sigma-Aldrich, St. Louis, MO).

Plasmid construction and protein purification

The lentiviral backbone plasmids FUW-mgp100, FUW-mTRP1, and FUW-mTRP2 were constructed by insertion of the cDNA of mouse melanoma antigen gp100 (mgp100), TRP1 (mTRP1), and TRP2 (mTRP2) into the

lentiviral backbone plasmid FUW downstream of the human ubiquitin C promoter. The αFAP-PE38 protein was purified as previously reported.[27] Briefly, the sequence encoding the truncated Pseudomonas exotoxin A (PE38) was cloned to the downstream portion of a sequence of species-crossreactive FAP-specific scFv (MO36)27 in the pET-28a(+) vector (Life Technologies, Grand Island, NY). The plasmids were transformed to the host *Escherichia coli* BL21 (DE3), which was then grown in Luria broth media containing 100 μg/ml of kanamycin at 37 °C. At an OD600 of 0.6, Isopropyl-β-D-thiogalactopyranoside (Sigma-Aldrich) was added to a final concentration of 1 mmol/l, and the culture was further incubated for 4 hours. Cells were harvested, and the recombinant protein was purified by applying it to a Ni2+IDA column (Qiagen, Valencia, CA).

Lentiviral vector production

To produce LV (LV-3Ag), the standard calcium phosphate precipitation procedure was used in the transient transfection of virus to produce cells for the LVs. HEK293T cells seeded in a 15-cm culture dish (BD Biosciences, San Jose, CA) were transiently transfected with lentiviral backbone plasmid (5 mg), packaging plasmids (pRRE, 2.5 mg; pRSV-REV, 2.5 mg), and the envelope plasmid pVSVG (2.5 mg) or pSVGmu (2.5 mg). Two days after transfection, the viral supernatant was collected and filtered through a 0.45-μm pore size filter (Nalgene, Rochester, NY). The supernatant was then ultracentrifugated at 25,000 rpm for 90 minutes, using an Optima L-90 K preparative ultracentrifuge and an SW28 rotor. The pellets were resuspended in an appropriate volume of cold Hank's balanced salt solution (Hyclone) for the intended *in vivo* study.

Immunization and tumor challenge study

For the prophylactic experiment, female C57BL/6 mice (n = 5 per group) were immunized with LV-3Ag at the indicated dosage. On day 14 postimmunization, the mice were challenged with the indicated number of B16-F10 cells s.c. on the right flank. Tumor growth was evaluated every other day by measuring tumor diameter with a caliper. Tumor volume was defined as (smallest diameter) × (longest diameter) × (height). For the therapeutic experiment, mice were challenged with the indicated number of B16-F10 cells s.c. on the right flank and immunized with LV-3Ag at day 3 post-tumor challenge. The αFAP-PE38 was administered to mice at the dose of 0.5 mg/kg via i.v. injection at day 7 postimmunization. Tumor volume was measured as described above. Survival end point was set when the tumor volume reached 2,000 mm^2.

Flow cytometry analysis

Tumor tissue from treated mice was harvested, minced to single suspension cells, filtered through 0.7 μm nylon strainers (BD Falcon, Franklin Lakes, NJ) and then purified by Percoll (Sigma-Aldrich) density-gradient separation. The purified cells were washed twice with cold PBS and then incubated for 10 minutes at 4 °C with rat anti-mouse CD16/CD32 mAbs (BD Biosciences) to block nonspecific binding. Cells were then stained with monoclonal antibodies conjugated with fluorescent dyes. All staining antibodies and isotype controls were purchased from eBioscience or BioLegend, including anti-CD45 (30-F11), anti-CD3 (145-2C11), anti-CD4 (RM4-5), anti-CD8 (53–6.7), anti-F4/80 (BM8), anti-CD206 (C068C2), anti-PD-1 (RMP1-30), anti-NK1.1 (PK136), anti-CD25 (PC61), anti-FoxP3 (FJK-16S), anti-CD11b (M1/70), anti-CD11c (N418), and anti-Gr-1 (RB6-8C5). Tregs were identified by $CD45^+CD4^+CD25^+$ $Foxp3^+$ markers; CD4 and CD8 T cells were identified by $CD45^+CD4^+$ and $CD45^+CD8^+$ markers, respectively. MDSCs were identified by $CD45^+CD11b^+Gr\text{-}1^+$ markers. Data were acquired on a MACSquant cytometer (Miltenyi Biotec, San Diego, CA), and the analysis was performed using FlowJo software (Tree Star, Ashland, OR).

Immunohistochemical and immunofluorescence analysis

Tumor tissues were excised and fixed with 4% formaldehyde for frozen sections. Acetone-fixed 5-μm sections were first treated with 0.3% hydrogen peroxide in PBS for 10 minutes to quench endogenous peroxidase. Nonspecific binding was blocked using PBS containing 10% serum. Sections were then incubated with rabbit anti-mouse Ki67 (Abcam, Cambridge, MA) in blocking buffer for 2 hours at room temperature, followed by incubation with horseradish peroxidase-conjugated anti-rabbit IgG secondary antibody (Santa Cruz Biotechnology, Santa Cruz, CA) for 30 minutes. After incubation, the slides were washed three times with PBS and then developed with 3, 3-diaminobenzidine substrate (Abcam). After substrate development, the sections were washed in water, counterstained with hematoxylin, dehydrated, and mounted with mounting medium (Richard-Allan Scientific). H&E staining and immunohistochemistry images were acquired by EVOS XL Cell Imaging System (Life Technologies, Carlsbad, CA). An *in situ* cell death detection kit (Roche, Indianapolis, IN) was used to detect apoptotic cells in the tumor area, following the manufacturer's instructions. The slides were analyzed with laser scanning by Nikon Eclipse Ti-E microscopy with a Yokogawa spinning-disk confocal scanner system (Solamere Technology Group, Salt Lake City, UT). Quantitation of the TUNEL- and Ki67-positive cells was performed using ImageJ software.

RNA isolation and transcripts analysis by qRT-PCR

Total tissue RNA was extracted from the flank tumor tissue using an RNeasy Mini Kit (Qiagen, Valencia, CA), according to the manufacturer's protocol. The cDNAs were synthesized from equal amounts of total RNAs using the High-Capacity RNA-to-cDNA Kit (Applied Biosystems, Grand Island, NY). Real-time qPCR with the appropriate primers was used to measure the expression of IL-2, IFN-γ, Perforin, Granzyme B, IL-12p35, IL-12p40, TRAIL, ICOS, TNF-α, and TGF-β genes. An ABI 7300 Real-Time PCR System (Applied Biosystems) was used for real-time qPCR to measure the incorporation of SYBR Green (Applied Biosystems). The $\Delta\Delta C_t$ method was used to calculate changes in gene expression level, and the raw values were normalized to the levels of GAPDH as a reference gene.

Statistical analysis

Statistical analysis was performed by GraphPad (Prism) software to determine *P* values by Student's *t*-test where two groups were compared. When more than two groups were compared, an analysis of variance with the Tukey post-test was used to determine significant differences between individual groups. Kaplan-Meier analysis was used to evaluate the survival of mice. A *P* value less than 0.05 was considered statistically significant, and data were presented as means ± standard error of the mean.

CONFLICT OF INTEREST

The authors declare no conflict of interest.

ACKNOWLEDGMENTS

This work was supported by National Institutes of Health grants (R01AI068978, R01CA170820, R01EB017206, and P01CA132681), a translational acceleration grant from the Joint Center for Translational Medicine, the National Cancer Institute (P30CA014089), and a grant from the Ming Hsieh Institute for Research on Engineering Medicine for Cancer.

REFERENCES

1. Girardet, C, Ladisch, S, Heumann, D, Mach, JP and Carrel, S (1983). Identification by a monoclonal antibody of a glycolipid highly expressed by cells from the human myeloid lineage. *Int J Cancer* **32**: 177–183.
2. Rosenberg, SA (1996). Development of cancer immunotherapies based on identification of the genes encoding cancer regression antigens. *J Natl Cancer Inst* **88**: 1635–1644.
3. Overwijk, WW, Tsung, A, Irvine, KR, Parkhurst, MR, Goletz, TJ, Tsung, K *et al.* (1998). gp100/pmel 17 is a murine tumor rejection antigen: induction of "self"-reactive, tumoricidal T cells using high-affinity, altered peptide ligand. *J Exp Med* **188**: 277–286.
4. Xiang, R, Lode, HN, Chao, TH, Ruehlmann, JM, Dolman, CS, Rodriguez, F *et al.* (2000). An autologous oral DNA vaccine protects against murine melanoma. *Proc Natl Acad Sci USA* **97**: 5492–5497.
5. Jäeger, E, Bernhard, H, Romero, P, Ringhoffer, M, Arand, M, Karbach, J *et al.* (1996). Generation of cytotoxic T-cell responses with synthetic melanoma-associated peptides in vivo: implications for tumor vaccines with melanoma-associated antigens. *Int J Cancer* **66**: 162–169.
6. Liu, Y, Peng, Y, Mi, M, Guevara-Patino, J, Munn, DH, Fu, N *et al.* (2009). Lentivector immunization stimulates potent CD8 T cell responses against melanoma self-antigen tyrosinase-related protein 1 and generates antitumor immunity in mice. *J Immunol* **182**: 5960–5969.
7. Yang, HG, Hu, BL, Xiao, L and Wang, P (2011). Dendritic cell-directed lentivector vaccine induces antigen-specific immune responses against murine melanoma. *Cancer Gene Ther* **18**: 370–380.

8. Rakhmilevich, AL, Imboden, M, Hao, Z, Macklin, MD, Roberts, T, Wright, KM *et al.* (2001). Effective particle-mediated vaccination against mouse melanoma by coadministration of plasmid DNA encoding Gp100 and granulocyte-macrophage colony-stimulating factor. *Clin Cancer Res* **7**: 952–961.
9. Salgaller, ML, Marincola, FM, Cormier, JN and Rosenberg, SA (1996). Immunization against epitopes in the human melanoma antigen gp100 following patient immunization with synthetic peptides. *Cancer Res* **56**: 4749–4757.
10. Mendiratta, SK, Thai, G, Eslahi, NK, Thull, NM, Matar, M, Bronte, V *et al.* (2001). Therapeutic tumor immunity induced by polyimmunization with melanoma antigens gp100 and TRP-2. *Cancer Res* **61**: 859–863.
11. Rosenberg, SA, Yang, JC and Restifo, NP (2004). Cancer immunotherapy: moving beyond current vaccines. *Nat Med* **10**: 909–915.
12. Curran, MA, Montalvo, W, Yagita, H and Allison, JP (2010). PD-1 and CTLA-4 combination blockade expands infiltrating T cells and reduces regulatory T and myeloid cells within B16 melanoma tumors. *Proc Natl Acad Sci USA* **107**: 4275–4280.
13. Zitvogel, L, Tesniere, A, Apetoh, L, Ghiringhelli, F and Kroemer, G (2008). [Immunological aspects of anticancer chemotherapy]. *Bull Acad Natl Med* **192**: 1469–87; discussion 1487.
14. Gulley, JL, Madan, RA and Arlen, PM (2007). Enhancing efficacy of therapeutic vaccinations by combination with other modalities. *Vaccine* **25 Suppl 2**: B89–B96.
15. Emens, LA and Jaffee, EM (2005). Leveraging the activity of tumor vaccines with cytotoxic chemotherapy. *Cancer Res* **65**: 8059–8064.
16. Chu, Y, Wang, LX, Yang, G, Ross, HJ, Urba, WJ, Prell, R *et al.* (2006). Efficacy of GM-CSF-producing tumor vaccine after docetaxel chemotherapy in mice bearing established Lewis lung carcinoma. *J Immunother* **29**: 367–380.
17. Machiels, JP, Reilly, RT, Emens, LA, Ercolini, AM, Lei, RY, Weintraub, D *et al.* (2001). Cyclophosphamide, doxorubicin, and paclitaxel enhance the antitumor immune response of granulocyte/macrophage-colony stimulating factor-secreting whole-cell vaccines in HER-2/neu tolerized mice. *Cancer Res* **61**: 3689–3697.
18. Sierro, SR, Donda, A, Perret, R, Guillaume, P, Yagita, H, Levy, F *et al.* (2011). Combination of lentivector immunization and low-dose chemotherapy or PD-1/PD-L1 blocking primes self-reactive T cells and induces anti-tumor immunity. *Eur J Immunol* **41**: 2217–2228.
19. Hodi, FS, Butler, M, Oble, DA, Seiden, MV, Haluska, FG, Kruse, A *et al.* (2008). Immunologic and clinical effects of antibody blockade of cytotoxic T lymphocyte-associated antigen 4 in previously vaccinated cancer patients. *Proc Natl Acad Sci U S A* **105**: 3005–3010.
20. Marx, J (2008). Cancer biology. All in the stroma: cancer's Cosa Nostra. *Science* **320**: 38–41.
21. Loeffler, M, Krüger, JA, Niethammer, AG and Reisfeld, RA (2006). Targeting tumor-associated fibroblasts improves cancer chemotherapy by increasing intratumoral drug uptake. *J Clin Invest* **116**: 1955–1962.
22. Bhowmick, NA, Neilson, EG and Moses, HL (2004). Stromal fibroblasts in cancer initiation and progression. *Nature* **432**: 332–337.
23. Wang, XM, Yao, TW, Nadvi, NA, Osborne, B, McCaughan, GW and Gorrell, MD (2008). Fibroblast activation protein and chronic liver disease. *Front Biosci* **13**: 3168–3180.
24. O'Brien, P and O'Connor, BF (2008). Seprase: an overview of an important matrix serine protease. *Biochim Biophys Acta* **1784**: 1130–1145.
25. Kraman, M, Bambrough, PJ, Arnold, JN, Roberts, EW, Magiera, L, Jones, JO *et al.* (2010). Suppression of antitumor immunity by stromal cells expressing fibroblast activation protein-alpha. *Science* **330**: 827–830.
26. Kalluri, R and Zeisberg, M (2006). Fibroblasts in cancer. *Nat Rev Cancer* **6**: 392–401.
27. Fang, J, Xiao, L, Joo, K-I, Liu, Y, Zhang, C, Liu, S *et al.* (2015). A potent immunotoxin targeting fibroblast activation protein for treatment of breast cancer in mice. *Int J Cancer* **138**: 1013–1023.
28. Gu-Trantien, C, Loi, S, Garaud, S, Equeter, C, Libin, M, de Wind, A *et al.* (2013). $CD4^+$ follicular helper T cell infiltration predicts breast cancer survival. *J Clin Invest* **123**: 2873–2892.
29. Fridman, WH, Pagès, F, Sautès-Fridman, C and Galon, J (2012). The immune contexture in human tumours: impact on clinical outcome. *Nat Rev Cancer* **12**: 298–306.
30. Brennen, WN, Isaacs, JT and Denmeade, SR (2012). Rationale behind targeting fibroblast activation protein-expressing carcinoma-associated fibroblasts as a novel chemotherapeutic strategy. *Mol Cancer Ther* **11**: 257–266.
31. Bui, JD, Uppaluri, R, Hsieh, CS and Schreiber, RD (2006). Comparative analysis of regulatory and effector T cells in progressively growing versus rejecting tumors of similar origins. *Cancer Res* **66**: 7301–7309.
32. Bates, GJ, Fox, SB, Han, C, Leek, RD, Garcia, JF, Harris, AL *et al.* (2006). Quantification of regulatory T cells enables the identification of high-risk breast cancer patients and those at risk of late relapse. *J Clin Oncol* **24**: 5373–5380.
33. Mandl, SJ, Rountree, RB, Dalpozzo, K, Do, L, Lombardo, JR, Schoonmaker, PL *et al.* (2012). Immunotherapy with MVA-BN®-HER2 induces HER-2-specific Th1 immunity and alters the intratumoral balance of effector and regulatory T cells. *Cancer Immunol Immunother* **61**: 19–29.
34. Chen, J, Zhang, L, Wen, W, Hao, J, Zeng, P, Qian, X *et al.* (2012). Induction of HCA587-specific antitumor immunity with HCA587 protein formulated with CpG and ISCOM in mice. *PLoS One* **7**: e47219.
35. Quezada, SA, Peggs, KS, Curran, MA and Allison, JP (2006). CTLA4 blockade and GM-CSF combination immunotherapy alters the intratumor balance of effector and regulatory T cells. *J Clin Invest* **116**: 1935–1945.
36. Lindau, D, Gielen, P, Kroesen, M, Wesseling, P and Adema, GJ (2013). The immunosuppressive tumour network: myeloid-derived suppressor cells, regulatory T cells and natural killer T cells. *Immunology* **138**: 105–115.
37. Anees, M, Horak, P, El-Gazzar, A, Susani, M, Heinze, G, Perco, P *et al.* (2011). Recurrence-free survival in prostate cancer is related to increased stromal TRAIL expression. *Cancer* **117**: 1172–1182.
38. Del Vecchio, M, Bajetta, E, Canova, S, Lotze, MT, Wesa, A, Parmiani, G *et al.* (2007). Interleukin-12: biological properties and clinical application. *Clin Cancer Res* **13**: 4677–4685.
39. Fewell, JG, Matar, MM, Rice, JS, Brunhoeber, E, Slobodkin, G, Pence, C *et al.* (2009). Treatment of disseminated ovarian cancer using nonviral interleukin-12 gene therapy delivered intraperitoneally. *J Gene Med* **11**: 718–728.
40. Jackaman, C, Bundell, CS, Kinnear, BF, Smith, AM, Filion, P, van Hagen, D *et al.* (2003). IL-2 intratumoral immunotherapy enhances CD8+ T cells that mediate destruction of tumor cells and tumor-associated vasculature: a novel mechanism for IL-2. *J Immunol* **171**: 5051–5063.
41. Ura, T, Okuda, K and Shimada, M (2014). Developments in Viral Vector-Based Vaccines. *Vaccines (Basel)* **2**: 624–641.
42. Gajewski, TF, Woo, SR, Zha, Y, Spaapen, R, Zheng, Y, Corrales, L *et al.* (2013). Cancer immunotherapy strategies based on overcoming barriers within the tumor microenvironment. *Curr Opin Immunol* **25**: 268–276.
43. Fotin-Mleczek, M, Zanzinger, K, Heidenreich, R, Lorenz, C, Kowalczyk, A, Kallen, KJ *et al.* (2014). mRNA-based vaccines synergize with radiation therapy to eradicate established tumors. *Radiat Oncol* **9**: 180.
44. Pinchuk, IV, Saada, JI, Beswick, EJ, Boya, G, Qiu, SM, Mifflin, RC *et al.* (2008). PD-1 ligand expression by human colonic myofibroblasts/fibroblasts regulates CD4+ T-cell activity. *Gastroenterology* **135**: 1228–1237, 1237.e1.
45. Nazareth, MR, Broderick, L, Simpson-Abelson, MR, Kelleher, RJ Jr, Yokota, SJ and Bankert, RB (2007). Characterization of human lung tumor-associated fibroblasts and their ability to modulate the activation of tumor-associated T cells. *J Immunol* **178**: 5552–5562.
46. Kakarla, S, Song, XT and Gottschalk, S (2012). Cancer-associated fibroblasts as targets for immunotherapy. *Immunotherapy* **4**: 1129–1138.
47. Nizar, S, Meyer, B, Galustian, C, Kumar, D and Dalgleish, A (2010). T regulatory cells, the evolution of targeted immunotherapy. *Biochim Biophys Acta* **1806**: 7–17.
48. Voron, T, Colussi, O, Marcheteau, E, Pernot, S, Nizard, M, Pointet, AL *et al.* (2015). VEGF-A modulates expression of inhibitory checkpoints on CD8+ T cells in tumors. *J Exp Med* **212**: 139–148.